Academic Journal of Science and Technology
ISSN: 2771-3032 | Vol. 11, No. 3, 2024

Fe-S Co-doped Porous Carbon Catalyzed Oxidation and Degradation of Dye Wastewater

Ziyu Wang [1], Yi Wang [1], Bo Xing [1], Fuping Zhang [1, *], Liang Jiang [1, *], Chao Gao [2], Kunbiao Tang [2]

[1] College of Chemical Engineering, Sichuan University of Science and Engineering, Zigong Sichuan, China
[2] Sichuan Honghua Industrial Co., Ltd., Leshan Sichuan, China

*** Corresponding Author:** Fuping Zhang and Liang Jiang

Abstract: In this paper, Fe-S co-doping method of "one-step blending + high temperature carbonization activation" was used to prepare highly efficient Fenton-like catalyst. Rhodamine B (Rh B) was used as the research object, and H_2O_2 was used as the oxidant to catalyze the oxidation and degradation of Rh B. The important process conditions (reaction pH, reaction temperature, H_2O_2 addition, catalyst addition) were optimized, and the reaction mechanism and stability of the catalyst were investigated. The experimental results show that the initial concentration of Rh B is 50 mg/L, n(Fe): n(S) = 1.8:1, C source 9 g; Under the conditions of reaction pH = 2, reaction temperature 50℃ and catalyst dosage 0.02 g, the degradation rate of Rh B can reach 91.17%. XRD, BET and FT-IR results show that the prepared catalyst has good pore structure and abundant functional groups on its surface. The kinetic results show that the oxidation and degradation of Rh B by Fe-S co-doped Fenton-like catalyst conforms to the quasi-first-order kinetic model. The experiment results of free radical quenching show that the reaction process is controlled by many kinds of free radicals. After repeated use for 3 times, the degradation rate of the catalyst decreased from 91.05% to 85.76%, and recovered to 88.32% after thermal regeneration, showing good repeatability and thermal stability.

Keywords: Fenton Reaction; Fe-S Co-doping; Porous Carbon; Dye Wastewater.

1. Introduction

As a typical coloring agent, dye has the characteristics of high toxicity, difficult degradation and so on, and has potential harm to the environment and human beings. Dye wastewater has become one of the typical refractory wastewater in recent years, so it is very important to accelerate the research of efficient and economical treatment methods [1].

Fenton-like oxidation technology catalyzes H_2O_2 chain reaction by Fe^{2+} to produce active free radicals with strong oxidation, thus efficiently treating organic pollutants. It has the advantages of simple operation, rapid reaction and wide application conditions. The key lies in how to prepare an efficient and stable Fenton-like catalyst[2].

Zero-valent Fe and Fe fund oxide are cheap and widely sourced, and are commonly used as active components of Fenton catalyst[3]. On the one hand, supported heterogeneous Fenton catalyst can make metal Fe stably and uniformly supported inside the carrier structure, on the other hand, it can also increase the specific surface area of the catalyst, thus significantly improving its reaction activity[4]. Due to its good electrical conductivity and adsorption properties, carbon material as a carrier of Fe-based catalyst can increase the active site of catalyst and facilitate the redox cycle of Fe^{2+}/Fe^{3+} [5, 6].

On the basis of Fe or Fe oxide alone, doping other elements can significantly improve the catalytic performance of the catalyst [7]. It is found that the S-doped modification process can produce bending, off-site and other structural defect sites on porous carbon materials, and increase the active site by changing the local surface electronic structure [8, 9]. These active sites can improve the electron transfer effect or adsorption or desorption between carbon materials and reactants, or enhance the interaction between carbon materials and metals, and improve the dispersion and stability of nano-metal particles [10]. This is due to the fact that by introducing elements to coordinate the formation of new structures, the electron transfer number can be increased to a large extent, and the apparent reactivity can be greatly improved [11]. Therefore, if S heteroatom can be introduced into Fe/C catalyst to form Fe-S co-doped porous carbon catalyst, the catalytic activity and stability of traditional Fe/C catalyst can be effectively improved [4, 12].

In this study, heterogeneous Fenton catalyst was prepared by the method of "one-step blending + high-temperature carbonization activation", and the important influencing conditions in the material preparation process were investigated, as well as the important technological conditions. The pH application range of the catalyst is expanded, the dissolution rate of iron ions is reduced, and the catalytic effect is finally improved. XRD, BET, FT-IR and other methods were used to characterize the structural and surface properties of the prepared catalyst, explore the relationship between Fe-S/AC structure and catalytic activity, explore the reaction mechanism of Fe-S/AC catalyst catalytic oxidation active factor and RhB removal, and fit the kinetic model according to the experimental results. Stability experiments were carried out to check the repeatability of the catalyst.

2. Experimental

2.1. Experimental Reagents and Instruments

Experimental reagents: anhydrous ferric chloride, L-cysteine, soluble starch, sodium chloride, nitric acid, H_2O_2, methanol, ethylenediamine tetraacetic acid, tert-butanol, ascorbic acid, Rh B, sodium hydroxide, all AR, and the experimental water was deionized water.

Experimental equipment: intelligent magnetic stirrer, electronic analysis balance, electric blast drying oven, UV-visible spectrophotometer, pH composite electrode,

circulating water multi-purpose vacuum pump, tube furnace.

2.2. Material Synthesis

Fe-S co-doped Fenton-like catalyst was prepared by "one-step blending + high temperature carbonization activation" method [13]. Anhydrous ferric chloride is the iron source, L-cysteine is the sulfur source, and starch is the carbon source. The specific steps are as follows: weigh 1.6g anhydrous ferric chloride, 10g soluble starch and 0.6g sodium chloride in a beaker, add about 100 mL of deionized water, and set the stirring in a blender at 1200 r/min and 80℃. After 1 h, add L-cysteine and stir continuously until thick. Pour the mixed goo into the surface dish and dry it in the oven at 90℃ for 12 h. Then calcination was carried out in the tube furnace, CO_2 was injected, the temperature was raised to 550℃ at 5℃/min, and then calcined for 2 h. The resulting black expanded solid is ground and transferred to the filter device, washed first to remove excess impurities, then pickled with 5% nitric acid for 12 h, and finally washed to neutral. After drying for 12 h, Fe-S co-doped Fenton-like catalyst is obtained, which is denoted as NFe-S/AC, where N is the value of n (Fe): n (S).

2.3. Materials Characterization

(1) XRD analysis: Bruker/D2 PHASER X-ray diffractometer of Bruker Company was used for analysis.

(2) BET analysis: The 3H-2000PS2 specific surface and aperture measuring instrument of Best Company was used for analysis.

(3) FT-IR analysis: Thermo Scientific NICOLET 6700 Fourier transform infrared spectrometer was used to identify active carbon functional groups.

2.4. Catalytic Oxidation Degradation of Rh B Experiment

Prepare 50 mg/L Rh B solution 200 mL in a beaker and start stirring at 50℃ and 1200 r/min. Add nitric acid to adjust pH, then add 2 mL H_2O_2. Sampling was performed at 0, 2, 5, 10, 20, 30, 40, 50, 60 min. The corresponding absorbance was measured, and the Rh B concentration was calculated using the fitted Rh B standard curve.

3. Result Analysis and Discussion

3.1. Catalyst Characterization Result

3.1.1. XRD Analysis

The crystal structures of different catalysts were characterized by X-ray diffraction (XRD). It can be seen from Fig.1 that the characteristic diffraction peak of S at 32.89° and Fe at 37.12° are the characteristic diffraction peaks [14]. After Fe and S co-doped, the characteristic diffraction peaks still exist on the catalyst, indicating that Fe and S have no effect on the crystal structure of porous carbon materials [15].1.5Fe-S/AC、1.8Fe-S/AC、2.0Fe-S/AC characteristic diffraction peaks corresponding to the supported Fe and S elements appear in the XRD patterns of the catalysts, while the corresponding characteristic diffraction peaks appear in the XRD patterns of 1.5Fe-S/AC catalysts, which may be due to too little iron oxide supported on the carrier surface. With the increase of n (Fe): n (S), the characteristic diffraction peak of the catalyst becomes more obvious, indicating that Fe and S elements are successfully loaded into the porous carbon.

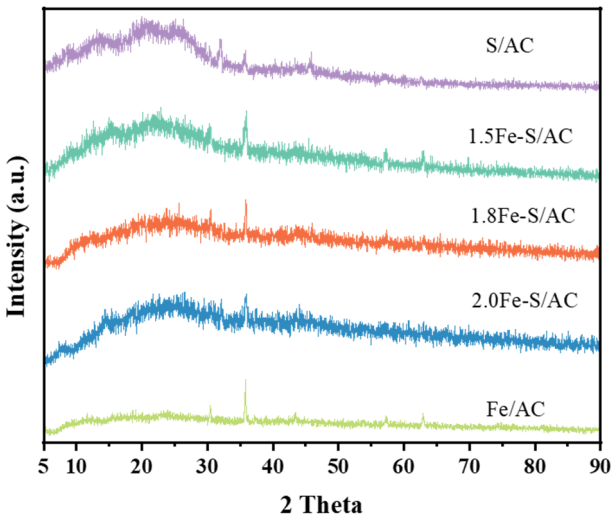

Figure 1. XRD Spectra of Fe-S/AC

3.1.2. BET Analysis.

The properties and number of active sites on the catalyst surface are the key factors affecting the catalytic activity, and a larger specific surface area is conducive to the generation and dispersion of active sites, and increasing the contact area can improve the catalytic efficiency [5, 16]. The N_2 adsorption/desorption test results of different Fe-S/AC catalysts are shown in Table 1. With the increase of Fe content, the specific surface area also increases gradually. This may be because the carbon material reacts with the iron source at high temperatures to form iron carbides, which can effectively promote the activation of carbon and generate more microporous and mesoporous structures [17, 18]. However, Fe/AC has the largest specific surface area, but its catalytic activity is weak, which indicates that other factors may affect its catalytic activity [14, 19],Therefore, other characterization methods were used to further analyze and study.

Table 1. Specific Surface Area and Pore Volume of Fe-S/AC

Catalyst	BET Surface Area [m^2g^{-1}]	Pore diameter [nm]	Pore Volume [$cm^{-3}g^{-1}$]
S/AC	106.66	3.03	0.0808
1.5Fe-S/AC	146.79	2.73	0.1003
1.8Fe-S/AC	179.14	2.17	0.0973
2.0Fe-S/AC	217.43	2.24	0.1526
Fe/AC	390.61	2.15	0.2103

3.1.3. FT-IR Analysis.

As shown in Fig.2, Fe-S/AC catalysts of different proportions were characterized by infrared spectroscopy and their surface functional groups were qualitatively analyzed. The wider absorption peak of 3475 cm^{-1} is caused by the -OH or -CH functional groups [20]. The absorption peak at 1123 cm^{-1} is caused by C-C, the absorption peak at 1625 cm^{-1} is caused by C=C, and the absorption peak at 3768 cm^{-1} belongs to the vibration peak of S-H [21]. Comparing different catalysts, it is found that the catalyst without S source does not have obvious vibration peak[22]. With the increase of S content, the vibration peak of S-H becomes more obvious, indicating that the addition of L-cysteine can successfully incorporate S element into the catalyst.

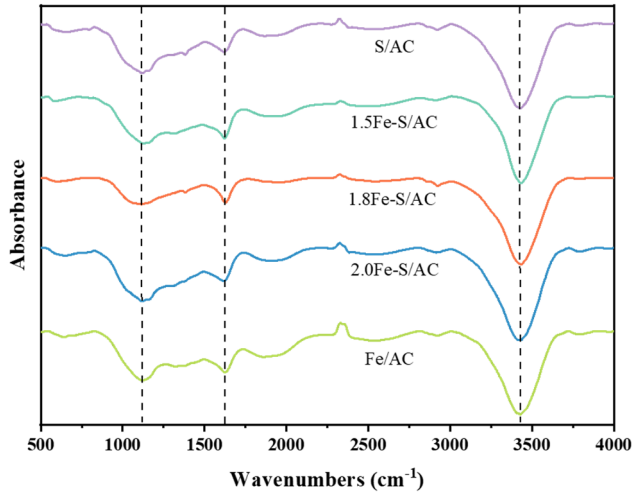

Figure 2. FT-IR Spectra Of Fe-S/AC

3.2. Catalyst Activity Evaluation

3.2.1. Catalyzed Oxidative Degradation Rh B Wastewater of Fe-S/AC.

Under the conditions of Rh B concentration of 50 mg/L, catalyst dosage of 0.1 g/L, solution pH = 4, and reaction temperature of 50 ℃, the results of catalytic oxidation of Rh B wastewater with different Fe-S/AC are shown in Fig.3. When only H_2O_2 is added, Rh B is almost not degraded, indicating that the oxidation of H_2O_2 is not enough to decompose Rh B [23]. Fe/AC and S/AC catalysts also showed the same results, indicating that a single active component could not catalyze the decomposition of H_2O_2 to generate active free radicals to degrade Rh B. The degradation rate of Fe-S/AC catalysts with different proportions is higher than that of single active component, indicating that Fe-S co-doping can improve the ability of catalytic material to activate H_2O_2. The degradation rate of 1.8Fe-S/AC was the highest, which increased from 64.14% when the load ratio was 1.5Fe-S/AC to 80.60% (1.8Fe-S/AC). This may be because with the increase of Fe sources, the catalyst produces more Fe-based active sites, which generates more active free radicals, helping to catalyze the reaction. However, the degradation rate decreased to 69.12% when Fe loading was further increased. This may be the result of less Fe^{2+} being loaded on a certain specific surface area [12].

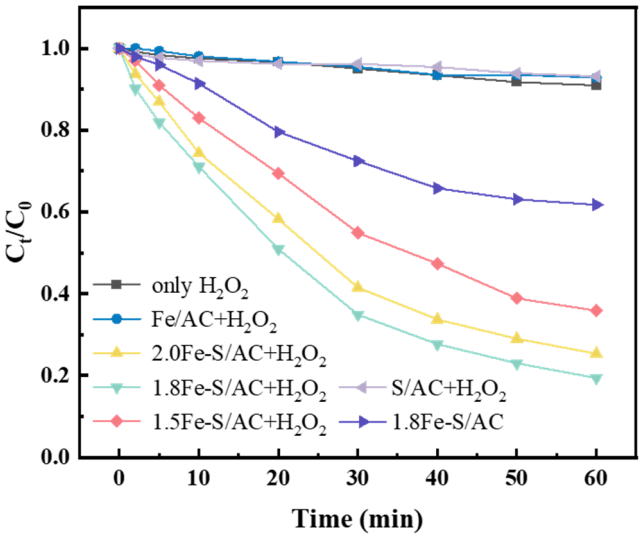

Figure 3. Fe-S/AC Catalyzed Oxidative Degradation of Rh B

3.2.2. Influence of C Source Addition.

Under the same experimental conditions above, the effects of different C source additions on the activity of Fe-S/AC catalyst were investigated, and the results were shown in Fig.4. The catalytic degradation effect is the best when the C source is 9 g. When the amount of C source is small, the degradation rate is 67.73%. It may be that the specific surface area of the prepared catalyst is not large enough, and the volume is not enough, resulting in poor catalytic adsorption effect [24]. When the C source was increased to 9 g, the degradation rate increased to 81.47%. However, when the addition of more C sources increases, the pore structure of the prepared catalyst may be blocked [25], resulting in a decline in the catalytic performance of the catalyst and a low degradation rate [26]. The addition of C source in catalyst preparation was determined to be 9 g.

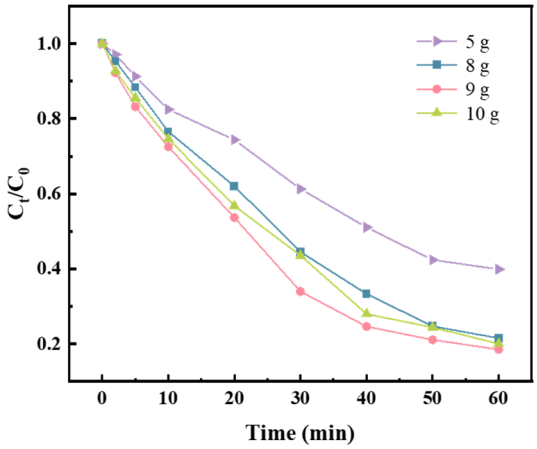

Figure 4. Fe-S/AC With Different C Sources Catalyzed The Oxidative Degradation Of Rh B

3.2.3. The Effect of Reaction Ph.

Based on the optimum preparation conditions, the effects of technological parameters on the H_2O_2 activation activity of Fe-S/AC catalyst were investigated. The influence rule of reaction pH is shown in Fig.5. The degradation effect of Rh B wastewater decreases with increasing pH [27]. When the pH increases from 4 to 8, the degradation rate decreases from 60.07% to 37.74%, which is because Fenton reaction needs to be carried out in an acidic environment [6]. When pH = 2, the degradation rate was 86.84%. This is due to the fact that the surface charge of the catalyst will be changed under acidic conditions, and the catalytic activity of the catalyst will be improved, thus improving the degradation efficiency of the catalyst for Rh B [28].

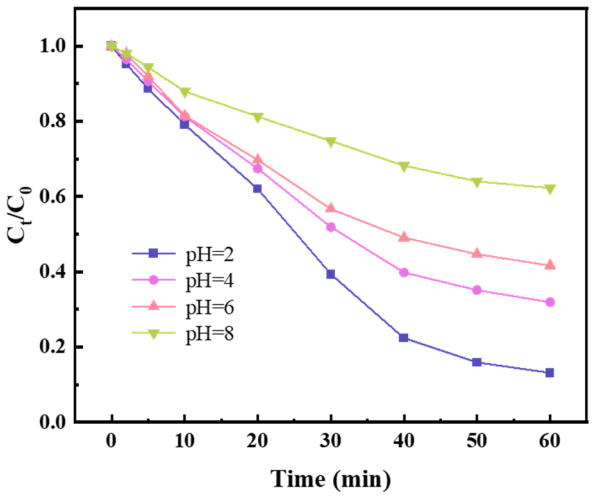

Figure 5. Fe-S/AC Catalyzed Oxidation and Degradation of Rh B At Different pH

3.2.4. The Effect of Reaction Temperature.

Reaction temperature also has a great impact on Fenton reaction. At a higher temperature, the reaction rate is faster, but more energy is consumed. The degradation rate of Rh B at different reaction temperatures is shown in Fig.6. When the reaction temperature increased from 40 ℃ to 60 ℃, the degradation rate of Rh B increased from 69.07% to 90.78%. This indicates that the higher the reaction temperature is, the more beneficial it is to increase the activity of the catalyst and facilitate the reaction [29]. This is mainly because the increase in temperature can accelerate the mass transfer efficiency between the substrate and the catalyst, resulting in an increase in the number of reactive activated molecules [25]. At the same time, because high temperature helps to produce more active free radicals, it can enhance its oxidation capacity, thus accelerating the reaction [30]. The increase of temperature will also accelerate the formation rate of •OH [31]. It can help •OH react with organic matter, effectively decompose refractory macromolecules into small molecules, and realize Rh B mineralization [32]. However, considering the cost and time of actual wastewater treatment, 50 ℃ was chosen as the temperature of catalytic oxidation experiment.

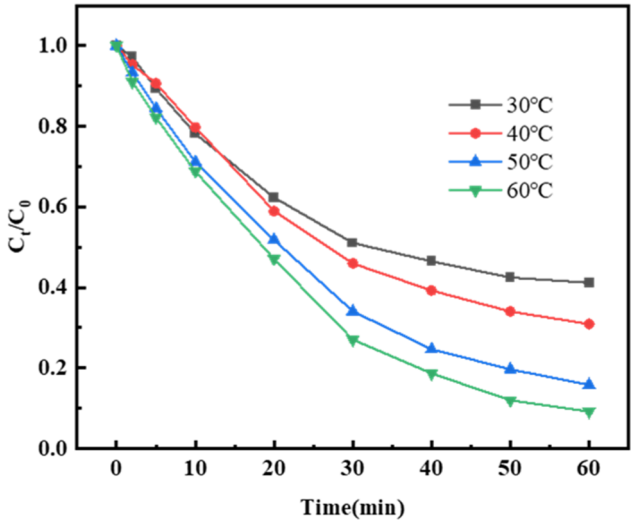

Figure 6. Fe-S/AC Catalyzed Oxidation and Degradation of Rh B At Different Tmperature

3.2.5. The Effect of Catalyst Addition.

As shown in Fig.7, when the amount of catalyst is 0.015 g, the degradation rate of Rh B is 75.35%. It may be that the amount of catalyst is too small, resulting in not enough active sites to catalyze oxidative degradation of Rh B wastewater. When the addition of catalyst increases from 0.02 g to 0.03 g, the degradation rate increases from 90.92% to 96.18%, and the degradation rate further increases, which may be because the increase of catalyst will enable enough Fe^{2+} and H_2O_2 in the solution to react to generate strong oxidizing •OH, thus rapidly degrading Rh B [33]. However, since the degradation rate has reached 90.92% at 0.02g, continuing to increase will not significantly improve the degradation rate, but also increase the cost, so the subsequent selection of catalyst addition is 0.02g.

In summary, the experimental results show that the initial concentration of Rh B is 50 mg/L, n(Fe): n(S)= 1.8:1, C source 9 g; Under the conditions of reaction pH = 2, reaction temperature 50℃ and catalyst dosage 0.02 g, the degradation rate of Rh B can reach 91.17%.

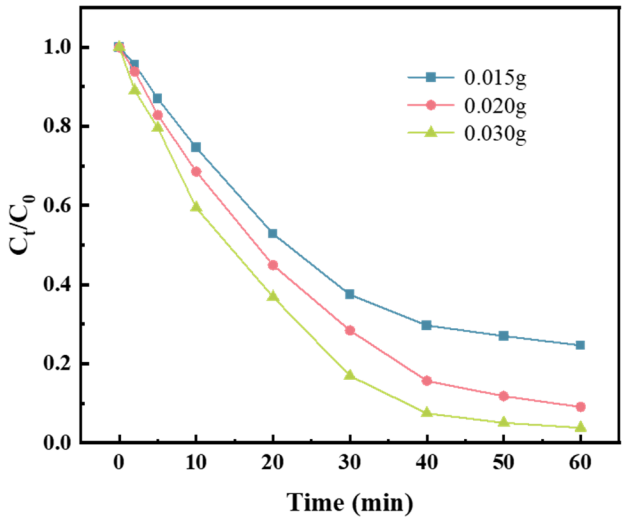

Figure 7. Fe-S/AC Catalyzed Oxidation and Degradation of Rh B Under Different Addition

3.2.6. Stability of Fe-S/AC Catalysts.

The experiment was carried out under the above optimal catalyst and optimal process conditions, and the reaction was repeated under the same operation, and the results were shown in Fig.8. After repeated use for 3 times, the degradation rate of Rh B wastewater decreased from 91.05% to 85.76%, but after one calcination, the degradation rate increased to 88.32%. After the third experiment, the degradation rate decreased slightly, which may be due to the fact that when Rh B reacted with the catalyst surface, a covering layer or physical adsorption layer would be formed on the catalyst surface. The residual covering of organic matter would reduce the specific surface area of the catalyst, resulting in some active sites on the catalyst surface being obscured, thus affecting the activity and selectivity of the catalyst. At the same time, impurities or pollutants in the reactants may also be deposited on the catalyst surface during the catalytic reaction, thus affecting the degradation effect of the catalyst [34]. The catalytic activity was partially recovered after calcination, which may be due to the fact that some small organic molecules covered the active site during the use of the catalyst and blocked the pore channels, thus resulting in the inactivation of porous carbon [10]. Through thermal regeneration treatment, the organic matter covering the active site can be shed and the catalytic activity can be restored.

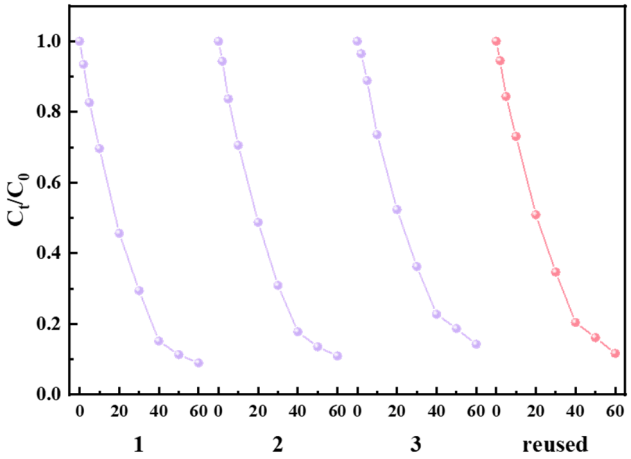

Figure 8. Stability Of 1.8Fe-S/AC

3.3. Dynamics Research

Taking Rh B as the research object, under the conditions of initial concentration of Rh B being 50 mg/L, pH = 2, volume

of H_2O_2 being 2 mL and catalyst being 0.02 g, the effect of reaction temperature on catalytic oxidative degradation of Rh B was studied and the Arrhenius curve was fitted, as shown in Fig.9. When the reaction temperature increased from 30 ℃ to 60 ℃, the degradation rate of Rh B increased from 58.11% to 91.78%. This is mainly due to the fact that the higher the temperature is, the more active free radicals are generated by thermal activation, thus accelerating the degradation of Rh B [26]. According to the quasi-first-order kinetic equation $C_t/C_0 = e^{-kt}$, the obtained temperature data were fitted, and the linear fitting correlation $R^2 > 0.97$ was obtained, indicating that the degradation rate of Rh B prepared at different reaction temperatures was in line with the quasi-first-order kinetic model [35]. The Arrhenius formula is used to calculate the reaction activation energy of 37.81 kJ/mol, which is lower than the corresponding activation energy when it is used as a catalyst, which confirms the good catalytic activity of the co-doped Fenton-like catalyst prepared in the experiment. It can be seen from kinetic analysis that S doping modification is an effective means to enhance its catalytic activity [36]. Combined with the characterization data, it can be seen that although it has the largest specific surface area, its catalytic activity is not optimal, indicating that the specific surface area is not the key factor affecting its activity, but mainly depends on the number and type of surface active functional groups [34].

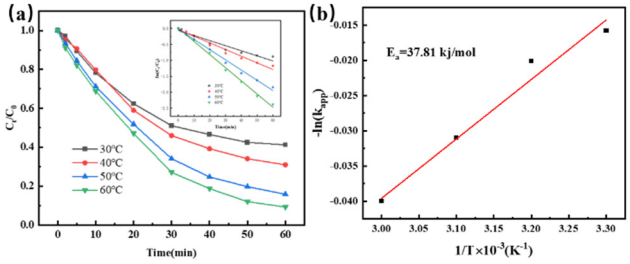

Figure 9. Dynamics Research Results Of 1.8Fe-S/AC

3.4. Reaction Mechanism

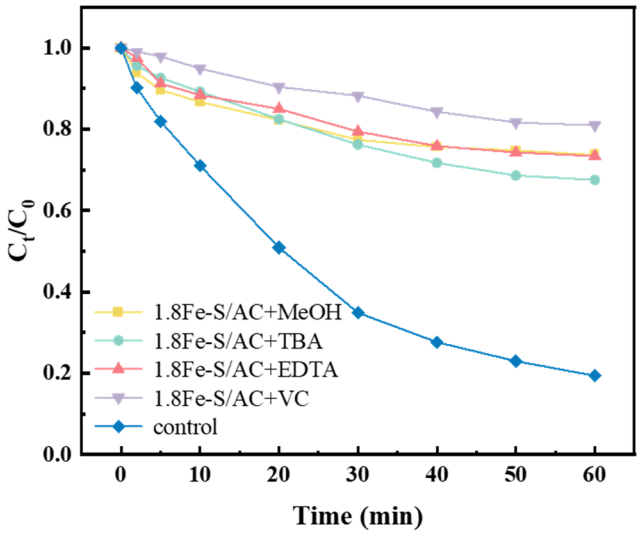

Figure 10. Reaction Mechanism Of 1.8Fe-S/AC

In order to explore the reaction mechanism of this process, different free radical masking agents were added in the reaction process, and 2mM MeOH, TBA, EDTA and VC were added respectively as •OH, SO4•⁻, $\cdot O_2^-$ and $^1O_2$ free radical quenching agents for masking experiments, as shown in Fig.10. After 60 min, the degradation rates of Rh B were 26.30%, 32.47%, 26.56% and 19.02%, respectively. After the quenching agent was added, the degradation rate decreased significantly, indicating that a variety of active free radicals co-existed in the process and jointly participated in the oxidative degradation process of Rh B, thus showing a good degradation rate [35, 37].

4. Summary

(1) The optimal experimental conditions are: n(Fe): n(S) = 1.8:1, C source 9 g; When pH = 2, reaction temperature 50 ℃ and catalyst dosage 0.02 g, the degradation rate of Rh B can reach 91.17% after 60 min. Compared with Fe and S alone, the catalyst supported by Fe and S has better degradation of Rh B wastewater, among which 1.8Fe-S/AC has the highest degradation rate and has good stability.

(2) XRD results show that S doping has no effect on the crystal structure. The BET results showed that the specific surface area increased with the increase of Fe content.

(3) The kinetic analysis results show that the degradation of Rh B by Fe-S co-doped Fenton-like catalyst conforms to the quasi-first-order kinetic model. The activation energy calculated by Arrhenius formula is 37.81 kJ/mol (> 29 kJ/mol), which belongs to the surface reaction control process.

(4) The results of free radical quenching show that a variety of active free radicals co-exist in the catalytic oxidation reaction system, indicating that the catalyst degradation of Rh B is an oxidation process dominated by free radicals.

CONFLICTS OF INTEREST

The authors declare that they have no conflict of interest.

Acknowledgments

Supported by The Innovation Fund of Postgraduate, Sichuan University of Science & Engineering, Y2022024; Sichuan Science and Technology Program, 2023NSFSC1118, 2024YFHZ0103, 2024NSFSC1112; Chenguang High Performance Fluorine Material Innovation Center, SCFY2204; Sichuan University of Science and Engineering, 2023RC05; Opening Project of Chemical Synthesis and Pollution Control Key Laboratory of Sichuan Province; CSPC202203, Returned Overseas Program of Sichuan University of Science and Engineering, 2021RC25.

References

[1] Wei Yin, Liu Yang, Wang Tianyi, Zhang Guojun, Yang Liwei, He Chuanshu, Xiong Zhaokun, Pan Zhicheng, Lai Bo. "N, S co-doped porous carbon to accelerate Fe3+/Fe2+ redox cycle for peroxymonosulfate activation", Separation and Purification Technology, Vol.328, pp.125080,2024. https://doi.org/ 10. 1016/ j. seppur.2023.125080.

[2] Zhang Junyuan, Deng Ziwei, Bai Shuli, Liu Changyu, Zhang Mengchen, Peng Chao, Xu Xiaolong, Jia Jianbo, Luan Tiangang. "Fe, N, S co-doped carbon network derived from acetate-modified Fe-ZIF-8 for oxygen reduction reaction", Journal of Colloid and Interface Science, Vol.658, pp.373-82,2024. https://doi.org/10.1016/j.jcis.2023.12.047.

[3] Zhang Pengfei, Chen Chen, Zhang Xiaohua, Jiang Zhigang, Huang Junlin, Chen Jinhua. "Fe and S co-doped N-enriched hierarchical porous carbon polyhedron as efficient non-noble-metal electrocatalyst toward oxygen reduction reaction in both alkaline and acidic medium", Electrochimica Acta,Vol.298, pp.570-9,2019. https://doi.org/ 10.1016/j. electacta. 2018. 12.119.

[4] Liu Yan, Liu Xiao-peng, Dai Ying, Wang Yun, Yuan Ding-zhong, Liu Jin-biao, Chew Jia-wei. "Preparation of a N, S, P co-doped and oxidized porous carbon for the efficient adsorption of uranium(VI)", New Carbon Materials, Vol.36, pp.1138-46,2021. https://doi.org/10.1016/S1872-5805(21) 600 55-0.

[5] Hu Xiwei, Sun Xun, Song Qiang, Zhu Yangyang, Long Yu, Dong Zhengping. "N,S co-doped hierarchically porous carbon materials for efficient metal-free catalysis", Green Chemistry, Vol.22, pp.742-52,2020. https://doi.org/ 10.1039/ C9GC 038 63A.

[6] Chen Yuyu, Liang Qianwei, Deng Yuhui, Bin Yuliang, Wang Tao, Luo Hanjin. "Peroxymonosulfate activation by concave porous S/N co-doped carbon: Singlet oxygen-dominated non-radical efficient oxidation of organics", Journal of Environmental Chemical Engineering,Vol.10, pp.107933,2022. https://doi.org/10.1016/j.jece.2022.107933.

[7] Lin Wujun, Lu Ying-Rui, Peng Wei, Luo Min, Chan Ting-Shan, Tan Yongwen. "Atomic bridging modulation of Ir–N, S co-doped MXene for accelerating hydrogen evolution",Journal of Materials Chemistry A, Vol.10, pp.9878-85,2022.https:// doi.org/ 10.1039/D2TA00550F.

[8] Chang Fangfang, Su Panpan, Guharoy Utsab, Ye Runping, Ma Yanfu, Zheng Huajun, Jia Yi, Liu Jian. "Edge-enriched N, S co-doped hierarchical porous carbon for oxygen reduction reaction", Chinese Chemical Letters, Vol.34, pp.107462,2023. https://doi.org/10.1016/j.cclet.2022.04.060.

[9] Chang Yingna, Li Jiawei, Zhang Tian, Wang Jindi, Wang Danni, Liu Yu, Yang Miaosen, Xing Rong, Zhang Guoxin. "Correlating oxygen reduction activity of N, S-co-doped carbon with the structures of dopant molecules", Journal of Alloys and Compounds, Vol.986, pp.174165,2024. https://doi. org/ 10.1016/j.jallcom.2024.174165.

[10] Li Zeyu, Gao Qiuming, Liang Xiao, Zhang Hang, Xiao Hong, Xu Peng, Liu Zhengping. "Low content of Fe3C anchored on Fe,N,S-codoped graphene-like carbon as bifunctional electrocatalyst for oxygen reduction and oxygen evolution reactions", Carbon, Vol.150, pp.93-100,2019.https:// doi.org/ 10. 1016/j.carbon.2019.05.012.

[11] Wang Yan, Wang Ying, Liu Yangxian. "Fe2+/heat-coactivated PMS oxidation-absorption system for H2S removal from gas phase",Separation and Purification Technology, Vol. 286, pp. 120458,2022. https://doi. org/ 10.1016/ j.seppur. 2022. 120458.

[12] Jeyalakshmi Velu, Mahalakshmy Rajaram, Krishnamurthy Konda Ramasamy, Viswanathan Balasubramanian."Strontium titanates with perovskite structure as photo catalysts for reduction of CO2 by water: Influence of co-doping with N, S & Fe",Catalysis Today,Vol.300,pp.152-9,2018. https://doi.org/ 10. 1016/j.cattod.2017.02.050.

[13] Guo Junxia, Niu Qijian, Yuan Yichun, Maitlo Inamullh, Nie Jun, Ma Guiping. "Electrospun core–shell nanofibers derived Fe–S/N doped carbon material for oxygen reduction reaction", Applied Surface Science, Vol.416, pp.118-23,2017. https://doi. org/ 10.1016/j.apsusc.2017.04.135.

[14] Huang Hsin-Chih, Lin Yu-Chuan, Chang Sun-Tang, Liu Chia-Chi, Wang Kai-Chin, Jhong Huan-Ping, Lee Jyh-Fu, Wang Chen-Hao. "Effect of a sulfur and nitrogen dual-doped Fe–N–S electrocatalyst for the oxygen reduction reaction", Journal of Materials Chemistry A,Vol.5, pp.19790-9,2017. https://doi. org/ 10.1039/C7TA05030E.

[15] Liu Dawei, Srinivas Katam, Chen Anran, Ma Fei, Yu Hesheng, Zhang Ziheng, Wang Mengya, Wu Yu, Chen Yuanfu. "Atomic Fe/Zn anchored N, S co-doped nano-porous carbon for boosting oxygen reduction reaction", Journal of Colloid and Interface Science, Vol.635,pp.578-87,2023. https://doi. org/ 10. 1016/j.jcis.2022.12.156.

[16] Feng Liping, Chang Yunzhen, Song Hua, Hou Wenjing, Li Yanping, Zhao Yun, Xiao Yaoming, Han Gaoyi. "N, S co-doped porous carbon with high capacitive performance derived from heteroatom doped phenolic resin", Journal of Electroanalytical Chemistry, Vol.908,pp. 116069, 2022. https: // doi.org/10.1016/j.jelechem.2022.116069.

[17] Li Bing, Xiang Tingting, Shao Yuqi, Lv Fei, Cheng Chao, Zhang Jiali, Zhu Qingchao, Zhang Yifan, Yang Juan. "Secondary-Heteroatom-Doping-Derived Synthesis of N, S Co-Doped Graphene Nanoribbons for Enhanced Oxygen Reduction Activity", Nanomaterials, Vol.12,pp.12457,2022. https://doi.org/10.3390/nano12193306.

[18] Tang Lin, Yue Ruifeng, Wang Yan. "N-type B-S co-doping and S doping in diamond from first principles", Carbon, Vol.130, pp.458-65,2018. https://doi.org/ 10.1016/j. carbon. 2018.01.028.

[19] Wu Lin, Wang Chong-Chen, Chu Hong-Yu, Yi Xiao-Hong, Wang Peng, Zhao Chen, Fu Huifen. "Bisphenol A cleanup over MIL-100(Fe)/CoS composites: Pivotal role of Fe–S bond in regenerating Fe2+ ions for boosted degradation performance", Chemosphere, Vol.280,pp.130659,2021. https://doi.org/ 10. 1016/ j.chemosphere.2021.130659.

[20] Yu Jiangfang, Tang Lin, Pang Ya, Zhou Yaoyu, Feng Haopeng, Ren Xiaoya, Tang Jing, Wang Jiajia, Deng Lifei, Shao Binbin. "Non-radical oxidation by N,S,P co-doped biochar for persulfate activation: Different roles of exogenous P/S doping, and electron transfer path", Journal of Cleaner Production, Vol.374, pp.133995,2022. https://doi.org/ 10.1016/j. jclepro. 2022. 133995.

[21] Zhang Tongtong, Cai Xiunan, Lin Xiangxuan, Jiang Zhaoming, Jin Hao, Huang Zuqiang, Gan Tao, Hu Huayu, Zhang Yanjuan. "Mechanical activation-enhanced doping and defect strategy to construct Fe–S co-doped carbon nitride for efficient photocatalytic tetracycline degradation and hydrogen evolution", Separation and Purification Technology, Vol.314, pp.123618,2023. https://doi.org/ 10.1016/j. seppur. 2023. 123 618.

[22] Jaiswal Aniruddha, Kumar Rajeev, Prakash Rajiv. "Iron/Iron Carbide (Fe/Fe3C) Encapsulated in S, N Codoped Graphitic Carbon as a Robust HER Electrocatalyst", Energy & Fuels,Vol.35, pp.16046-53,2021. https://doi. org/10. 1021/ acs. energyfuels. 1c02125.

[23] Karuppiah Chelladurai, Venkatesh Krishnan, Arunachalam Prabhakarn, Ramaraj Sayee Kannan, Al-Mayouf Abdullah M., Yang Chun-Chen."Optimization of S-dopant on N, S co-doped graphene/CNT-Fe3C nanocomposite electrode for non-enzymatic H2O2 sensor",Materials Letters, Vol.285,pp. 129001, 2021.https://doi.org/10.1016/j.matlet.2020.129001.

[24] Wang Xuechun, Zhuang Yuan, Zhang Jia, Song Laizhou, Shi Baoyou. "Pollutant degradation behaviors in a heterogeneous Fenton system through Fe/S-doped aerogel", Science of The Total Environment, Vol.714, pp.136436, 2020. https:// doi.org/ 10. 1016/j.scitotenv.2019.136436.

[25] Li Zhifang, Yang Huimin, Zhang Dingding, Zhou Wenjing, Gao Nan, Wang Jiaxin, Yang Donghua. "Effects of Bi and S co-doping on the enhanced photoelectric performance of ZnO: Theoretical and experimental investigations", Journal of Alloys and Compounds, Vol.872, pp.159648,2021. https://doi. org/ 10. 1016/j.jallcom.2021.159648.

[26] Wang Weixia, Chen Jie, Wang Dake, Shen Yanmei, Yang Like, Zhang Tuo, Ge Jia. "Facile synthesis of biomass waste-derived fluorescent N, S, P co-doped carbon dots for detection of Fe3+ions in solutions and living cells", Analytical Methods, Vol.13,pp.789-95,2021. https://doi.org/10.1039/D0AY02186E.

[27] Ding Chunlu, Liu Zhen, Xiao Xiaolong, Li Jin, Li Qian. "Facile tuning Non-radical/Radical oxidation by nitrogen doping on Fe-S doped carbonaceous catalysts for peroxymonosulfate

activation", Separation and Purification Technology, Vol.337, pp.126359,2024. https://doi. org/10. 1016/j. seppur. 2024. 126 359.

[28] Long Yangke, Li Shun, Su Yiping, Wang Shuyang, Zhao Shiyin, Wang Shubin, Zhang Zhen, Huang Wei, Liu Yong, Zhang Zuotai. "Sulfur-containing iron nanocomposites confined in S/N co-doped carbon for catalytic peroxymonosulfate oxidation of organic pollutants: Low iron leaching, degradation mechanism and intermediates", Chemical Engineering Journal, Vol.404, pp.126499,2021. https://doi.org/10.1016/j.cej.2020.126499.

[29] Kavitha V., Ramesh P. S., Geetha D. "Synthesis and characterization of copper (Cu)/sulfur (S) co-doped anatase TiO2 via sol–gel method and photo degradation efficiency", Journal of Materials Science: Materials in Electronics, Vol.27, pp.8118-25,2016. https://doi.org/10.1007/s10854-016-4813-x.

[30] Altalhi Tariq, Mezni Amine, Aldalbahi Ali, Alrooqi Arwa, Attia Yasser, Santos Abel, Losic Dusan. "Fabrication and characterisation of sulfur and phosphorus (S/P) co-doped carbon nanotubes", Chemical Physics Letters, Vol.658, pp.92-6,2016. https://doi.org/10.1016/j.cplett.2016.06.028.

[31] Gao Yilong, Kang Limin, Lian Yajuan, Xin Weili, Wang Rongrong, Liang Jinhu, Zhang Lisa, Wang Duan, Xu Sailong. "In-situ sulfuration synthesis of N,S-doped carbon nanosheet encapsulated Fe-doped Co9S8 as anodes for tunable lithium storage", Applied Surface Science, Vol.473, pp.673-80,2019. https:// doi.org/10.1016/j.apsusc.2018.12.188.

[32] Razmjooei Fatemeh, Singh Kiran Pal, Yang Dae-Soo, Cui Wei, Jang Yun Hee, Yu Jong-Sung. "Fe-Treated Heteroatom (S/N/B/P)-Doped Graphene Electrocatalysts for Water Oxidation", ACS Catalysis, Vol.7, pp.2381-91,2017. https://doi. org/10.1021/acscatal.6b03291.

[33] Dib K., Trari M., Bessekhouad Y. "(S,C) co-doped ZnO properties and enhanced photocatalytic activity", Applied Surface Science, Vol.505, pp.144541,2020. https://doi. org/ 10. 1016/j.apsusc.2019.144541.

[34] Guo Minmin, Yang Huimin, Gao Mengting, Zhang Erhui, Liang Zhenhai, Han Peide. "Enhanced photoelectric performance of (2Al, S) co-doped rutile SnO2", RSC Advances,Vol.7,pp.42940-5,2017. https://doi.org/ 10.1039/ C7 RA07891A.

[35] Gao Nan, Gao Lilin, Yu Hongyu. "First-principles study of N and S co-doping in diamond", Diamond and Related Materials, Vol.132, pp.109651,2023. https://doi.org/ 10.1016/ j. diamond. 2022. 109651.

[36] Ganesan Peramaiyan, Gantepogu Chandra Shekar, Duraisamy Sidharth, Meledath Valiyaveettil Suneesh, Tsai Wei-Han, Hsing Cheng-Rong, Lin Kung-Hsuan, Chen Kuei-Hsien, Chen Yang-Yuan, Wu Maw-Kuen. "Carrier optimization and reduced thermal conductivity leading to enhanced thermoelectric performance in (Mg, S) co-doped AgSbTe2", Materials Today Physics, Vol.42, pp.101358,2024. https://doi. org/10. 1016/j.mtphys.2024.101358.

[37] Zhang Mei, Xu You, Zhang Hugang, Duan Zhongyao, Ren Tianlun, Wang Ziqiang, Li Xiaonian, Wang Liang, Wang Hongjing. "Synergistic coupling of P-doped Pd4S nanoparticles with P/S-co-doped reduced graphene oxide for enhanced alkaline oxygen reduction", Chemical Engineering Journal, Vol.429, pp.132194,2022. https://doi. org/10. 1016/j. cej. 2021.132194.